Excitonic Phases from Weyl Semimetals

Huazhou Wei, Sung-Po Chao, and Vivek Aji
Department of Physics and Astronomy, University of California, Riverside, California 92521, USA
(Received 20 July 2012; published 9 November 2012)

Systems with strong spin-orbit coupling, which competes with other interactions and energy scales, offer a fertile playground to explore new correlated phases of matter. Weyl semimetals are an example where the phenomenon leads to a low-energy effective theory in terms of massless linearly dispersing fermions in three dimensions. In the absence of interactions chirality is a conserved quantum number, protecting the semimetallic physics against perturbations that are translationally invariant. In this Letter we show that the interplay between interaction and topology yields a novel chiral excitonic insulator. The state is characterized by a complex vectorial order parameter leading to a gapping out of the Weyl nodes. A striking feature is that it is ferromagnetic, with the phase of the order parameter determining the direction of the induced magnetic moment.

DOI: 10.1103/PhysRevLett.109.196403 PACS numbers: 71.35.−y, 71.45.Lr

The emergence of materials whose properties are strongly influenced by spin-orbit coupling is an exciting new phenomenon in condensed matter physics. Topological insulators [1,2] and Weyl semimetals [3–6] are two canonical examples, where the degrees of freedom, describing the low-energy physics of a nonrelativistic many body system, are linearly dispersing massless fermions. An interesting possibility in these materials is the emergence of new phases of matter [7,8]. In this Letter we focus on the charge density wave (CDW) and excitonic insulating (EI) states in Weyl semimetals.

In three dimensions touching of nondegenrate bands is known to be stable. The dispersion near theses points is linear in momentum and the excitations satisfy the Weyl equation, a two component analog of the Dirac equation. Each node has a specific chirality, and a gapping of the nodes is possible only if nodes of opposite chirality hybridize. In other words, intranodal interactions cannot open a gap. This is in sharp contrast with graphene, a two-dimensional systems with nodes in the dispersion, where intranodal perturbation that breaks inversion or time reversal symmetry makes the excitations massive. The existence of Weyl points is responsible for new phenomena, such as large magnetoconductivity, the Adler-Bell-Jackiw anomaly, and anomalous Hall effect [4,8–11].

For Weyl semimetals to be realized the bands need to be nondegenerate. This is typically achieved by the breaking of time reversal symmetry. In real materials the Weyl points always occur in pairs with opposite chirality [9]. If inversion is also preserved, every Weyl node at $\vec{K}$ is accompanied by one with opposite chirality at $-\vec{K}$. The key is to find or identify systems where such nodes exist. Several candidates have emerged over the past two years. Weyl fermions are conjectured to be the low-energy excitations of pyrochlore irradiates (PIs) [3], topological normal insulator (TNI) heterostructures [4,5], and staggered flux states in a cold atom system [6]. While the physics of Weyl fermions has been extensively studied in the context of liquid ^{3}He [12,13], where they arise in the A phase, the recent developments have renewed searches for other systems that realize the phenomena [14].

The number of Weyl nodes varies from system to system. In the case of PIs, 24 nodes at symmetry related points are conjectured to exist [3] while the TNI heterostructures have two such nodes [4]. In both cases there is perfect nesting. Consequently, we seek to address the question of the possible particle-hole instabilities promoted by repulsive interactions. Even for local density density interactions, the chiral nature of the Weyl fermions leads to a number of different phases, only one of which opens a gap at the nodes. Before we explore the energetics of the possible phases, we summarize the physics of this gapped state.

To highlight the physics of the novel new state, we simplify to the case of two Weyl nodes and local density density interactions. A more general analysis including the effects of long-range Coulomb will be reported elsewhere. There are two types of particle-hole excitations that can arise in this case: (i) intranodal (occurring at zero momentum) and (ii) internodal (occurring at a finite fixed momentum associated with the nesting vector). These are excitonic phases [15], the former being the EI while the latter is the CDW. Unlike conventional condensates in these sectors, the electron hole pairing of Weyl fermions leads to chiral phases. A minimum interaction strength is required to nucleate them, which is the consequence of the vanishing density of states at the node. For local interactions, the chiral EI has the lowest threshold, opens a gap at the nodes, and is the most stable state. The sign of the gap is opposite at the two nodes, preserving inversion symmetry.

To characterize the broken symmetry state we define an orthonormal basis for three dimensional space $\{\hat{l}, \hat{m}, \hat{n}\}$. In particular, for the Cartesian coordinate system with $\hat{z}$ as the

quantization axis, the ordered state is one with $\langle \sum_{\vec{k}} \hat{e}^2_{\vec{k}} (c^{L\dagger}_{\vec{k},+} c^{L}_{\vec{k},-} - c^{R\dagger}_{\vec{k},+} c^{R}_{\vec{k},-}) \rangle = \Delta(\frac{\hat{x} \pm \imath \hat{y}}{\sqrt{2}}) \exp(\imath\chi)$, where $c^{L,R}_{\vec{k},\pm}$ is the fermion annihilation operator at the two Weyl nodes, labeled L and R, at momentum $\vec{k}$ in the band labeled $\pm$, $\hat{e}^2_{\vec{k}} = \{-\hat{k}_y/\sqrt{\hat{k}_x^2 + \hat{k}_y^2}, \hat{k}_x/\sqrt{\hat{k}_x^2 + \hat{k}_y^2}, 0\}$, Δ is the magnitude, and χ is the phase of the order parameter. The loss of rotational invariance is reflected in the vector $\hat{e}^2_{\vec{k}}$ appearing in the order parameter. In general it is a vector lying in the plane spanned by $\hat{l}$ and $\hat{m}$ (i.e., $\hat{e}^2_{\vec{k}} = \hat{n} \times \hat{k}/|\hat{n} \times \hat{k}|$, with $\hat{n} = \hat{l} \times \hat{m}$), and the corresponding order parameter is $\Delta(\frac{\hat{l} \pm \imath \hat{m}}{\sqrt{2}}) \exp(\imath\chi)$. Thus the order parameter breaks SO(3) × SO(3) × U(1) symmetry corresponding to spatial rotational (choice of the coordinates system $\{\hat{l}, \hat{m}, \hat{n}\}$), internal rotational (choice of $\hat{e}^2_{\vec{k}}$), and phase invariance (χ). This is in addition to the time reversal symmetry broken by the parent state.

The order parameter does not break inversion symmetry. Therefore the spin orientations for electrons at momentum $\vec{k}$ and $-\vec{k}$ are identical. The effect of the symmetry breaking is to cant spins in momentum space along a direction determined by the phase of the order parameter. Thus, vortex lines, if stabilized, in this system have an associated spin texture with finite divergence.

Model.—Consider a system with two Weyl nodes at $\vec{K}_0 = K_0 \hat{x}$ (labeled R) and $-\vec{K}_0 = -K_0 \hat{x}$ (labeled L) with chiralities $+1$ and -1, respectively. The Hamiltonian is $H_{0\pm} = \pm \hbar v \sum_{\vec{k}} \psi^\dagger_{\vec{k}\alpha} \vec{\sigma}_{\alpha\beta} \cdot (\vec{k} \mp \vec{K}_0) \psi_{\vec{k}\beta}$, where v is the Fermi velocity and $\vec{\sigma} = \{\sigma_x, \sigma_y, \sigma_z\}$ is a vector of Pauli matrices. The dispersion at each node is $\epsilon_{\vec{q}} = \pm \hbar v |\vec{q}|$ centered around $\pm \vec{K}_0$, with $\vec{q} = (\vec{k} \mp \vec{K}_0)$. The conduction (valence) band at the R node has its spin parallel (antiparallel) to $\vec{q}$, while the opposite is true at the L node. The general particle-particle interaction, in momentum space, takes the form

$$V = \sum_{\sigma,\sigma'} \sum_{\vec{k},\vec{k}',\vec{q}} V(\vec{q}) \psi^\dagger_{\vec{k}'+\vec{q},\sigma'} \psi_{\vec{k}',\sigma'} \psi^\dagger_{\vec{k}-\vec{q},\sigma} \psi_{\vec{k},\sigma}. \quad (1)$$

For the moment we do not make any assumptions on the nature of the interactions. Since the Weyl physics is the low-energy description of a more general theory, we enforce an upper cutoff in the momentum integrals (up to an energy Λ) around the Weyl point.

Particle-hole instabilities.—We rewrite the interaction in the basis of the noninteracting bands. Define $\psi^{R,L}_{\vec{q},\pm} = \eta^{R,L}_{\vec{q},\pm} c^{R,L}_{\vec{q},\pm}$ as the fermionic field of the four bands, where η is the spinor and c is the fermion annihilation operator. Of the 16 possible terms from Eq. (1) only six terms satisfy momentum conservation for scattering restricted to the states within the cutoff around the node. For every momentum $\vec{q} = q\hat{q}$, where $\hat{q} = \{\hat{q}_x, \hat{q}_y, \hat{q}_z\}$ is the unit vector along $\vec{q}$, we define two orthogonal vectors $\hat{e}^1_{\vec{q}} \equiv \hat{\theta}_{\vec{q}} = \{\hat{q}_x \hat{q}_z/\sqrt{\hat{q}_x^2 + \hat{q}_y^2}, \hat{q}_y \hat{q}_z/\sqrt{\hat{q}_x^2 + \hat{q}_y^2}, -\sqrt{\hat{q}_x^2 + \hat{q}_y^2}\}$ and $\hat{e}^2_{\vec{q}} \equiv \hat{\phi}_{\vec{q}} = \{-\hat{q}_y/\sqrt{\hat{q}_x^2 + \hat{q}_y^2}, \hat{q}_x/\sqrt{\hat{q}_x^2 + \hat{q}_y^2}, 0\}$, such that $\hat{q}$, $\hat{e}^1_{\vec{q}}$, and $\hat{e}^2_{\vec{q}}$ form a right-handed coordinate system (see Fig. 1). The unit sphere is spanned by the vector $\hat{q}$ by two rotations, one about any axis perpendicular to $\hat{e}^2_{\vec{q}}$ and the another about $\hat{e}^2_{\vec{q}}$. Construction above holds for an arbitrary quantization axis $\hat{n}$, with the corresponding polar and azimuthal angle for $\vec{q}$ defined in the coordinate frame $\{\hat{l}, \hat{m}, \hat{n}\}$. In the rest of the Letter we use the $\{\hat{x}, \hat{y}, \hat{z}\}$ coordinate system.

Specializing to potentials that are even functions of $\vec{k}$, i.e., $V(\vec{k}) = V(-\vec{k})$, the interaction in terms of $\hat{e}_{\vec{k}} = \hat{e}^1_{\vec{k}} + \imath \hat{e}^2_{\vec{k}}$ is

$$\begin{aligned} V = -\sum_{\vec{k},\vec{k}',n=\pm} \Bigg[& \frac{V(\vec{k}-\vec{k}')}{4} (\hat{e}_{\vec{k}} \cdot \hat{e}^*_{\vec{k}'} + \hat{e}^*_{\vec{k}} \cdot \hat{e}_{\vec{k}'}) \\ & \times \sum_{\tau=R,L} c^{\tau\dagger}_{\vec{k},n} c^{\tau}_{\vec{k},-n} c^{\tau\dagger}_{\vec{k}',-n} c^{\tau}_{\vec{k}',n} + \frac{V(\vec{k}-\vec{k}'-2\vec{K}_0)}{2} \\ & \times (\hat{e}_{\vec{k}} \cdot \hat{e}_{\vec{k}'} + \hat{e}^*_{\vec{k}} \cdot \hat{e}^*_{\vec{k}'}) c^{L\dagger}_{\vec{k},n} c^{L}_{\vec{k},-n} c^{R\dagger}_{\vec{k}',-n} c^{R}_{\vec{k}',n} \\ & - [2V(2\vec{K}_0) - V(\vec{k}-\vec{k}')(\hat{k} \cdot \hat{k}' + 1)] \\ & \times c^{L\dagger}_{\vec{k},n} c^{R}_{\vec{k},-n} c^{R\dagger}_{\vec{k}',-n} c^{L}_{\vec{k}',n} \Bigg]. \end{aligned} \quad (2)$$

The first and second term promote intranodal order with $\langle \sum_{\vec{k}} \vec{A}_{\vec{k}} c^{\tau\dagger}_{\vec{k},n} c^{\tau}_{\vec{k},-n} \rangle \neq 0$ ($\vec{A}_{\vec{k}}$ is an odd function of $\vec{k}$), while the last term leads to internodal order with $\langle \sum_{\vec{k}} \vec{A}_{\vec{k}} c^{\tau\dagger}_{\vec{k},n} c^{\bar{\tau}}_{\vec{k},-n} \rangle \neq 0$. In the rest of this Letter we analyze the possible symmetry broken states. These are dictated by the fact that (i) $\vec{A}_{\vec{k}}$ is one of three possible vectors $\{\hat{q}, \hat{e}^1_{\vec{q}}, \hat{e}^2_{\vec{q}}\}$, (ii) rotational invariance is broken, and (iii) the state is either polar or chiral in nature. These lead to eight possible candidates summarized in Table I.

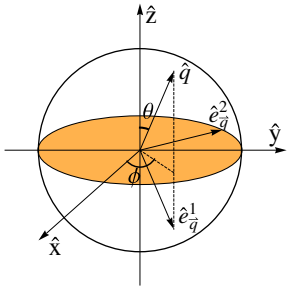

FIG. 1 (color online). The interaction shown in Eq. (2) is a function of three vectors ($\hat{q}$, $\hat{e}^1_{\vec{q}}$, and $\hat{e}^2_{\vec{q}}$) that form a right-handed coordinate system. Each vector couples to an operator of distinct symmetry in the particle-hole channel.

TABLE I. Possible excitonic phases, their symmetries, whether they gap out the Weyl node or not and the critical coupling g_c in units of $(\hbar v)^3/2\pi\Lambda^2$. Some g_c are evaluated analytically while others are obtained numerically. See Supplemental Material [16] for the details.

$\vec{A}_{\hat{k}}$	State	$\langle\vec{A}_k\rangle \propto$	Spectrum	g_c
$\hat{k}$	Chiral	$\hat{x}+i\hat{y}$	Gapless	3
	Polar	$\hat{z}$	Gapless	3
$\hat{e}^1_{\vec{k}}$	Chiral z	$\hat{x}+i\hat{y}$	Gapless	6
	Polar z	$\hat{z}$	Gapless	3
	Polar x	$\hat{x}$	Gapless	12
	Chiral x	$\hat{y}+i\hat{z}$	Gapless	4.8
$\hat{e}^2_{\vec{k}}$	Polar	$\hat{x}$	Gapless	4
	Chiral	$\hat{x}+i\hat{y}$	Gapped	2

Internodal charge density wave.—We begin by studying the internodal instability that establishes ordering at $2\vec{K}_0$ [third term in Eq. (2)]. For momentum independent interaction potentials, $V(\vec{k}) = g/\Omega$, where Ω is the volume of the system, the coupling takes the form

$$V_{\text{eff}} = -\frac{g}{\Omega}\sum_{\vec{k},\vec{k}'}\sum_{n=\pm}(\hat{k}c^{L\dagger}_{\vec{k},n}c^{R}_{\vec{k},-n})\cdot(\hat{k}'c^{R\dagger}_{\vec{k}',-n}c^{L}_{\vec{k}',n}). \quad (3)$$

Equation (3) is identical to that of the interaction in ^{3}He in the particle-particle channel that leads to chiral superfluidity [12,13]. In Weyl semimetals the corresponding state in the particle-hole channel is a CDW. Within mean field there are two possible instabilities: (i) chiral CDW, $\vec{\Delta}_c = \frac{g}{\Omega}\langle\sum_{\vec{k}'}\hat{k}'c^{\tau\dagger}_{\vec{k}',n}c^{\bar{\tau}}_{\vec{k}',-n}\rangle = \Delta_c(\frac{\hat{x}+i\hat{y}}{\sqrt{2}})$, and (ii) polar CDW, $\vec{\Delta}_p = \frac{g}{\Omega}\langle\sum_{\vec{k}'}\hat{k}'c^{\tau\dagger}_{\vec{k}',n}c^{\bar{\tau}}_{\vec{k}',-n}\rangle = \Delta_p\hat{z}$. Note that the directions chosen for the ground state are for convenience and all others that are obtained by rotation in three dimensions are equivalent. The former is a chiral state while the latter is a nonchiral p-wave CDW.

In Fig. 2 the zero temperature free-energy difference between condensate and normal states, denoted as E_c or condensation energy in the figure, and magnitude of the order parameter of the two states are plotted as a function

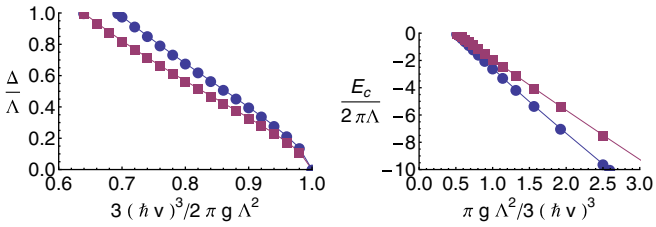

FIG. 2 (color online). Left: Order parameter magnitude as a function of inverse of the interaction strength for chiral (blue ○) and polar (purple □) CDW states. Right: Comparison of condensate energy E_c with $\mu = 0$ for aforementioned states as a function of the interaction strength.

of the interaction strength (details are available in the Supplemental Material). The two states have the same instability threshold. The magnitude of the order parameter is larger for the chiral state as compared to the polar state for the same interaction strength, leading to a greater (more negative) condensation energy for the former. Thus in this sector the lowest energy state is the chiral CDW.

The dispersion in the symmetry broken state is $E_{\vec{k}} = \sqrt{(\hbar v|\vec{k}|)^2 + |\vec{\Delta}_{c/p}\cdot\hat{k}|^2}$. The energy vanishes at the nodes and the Weyl points are preserved. This is remarkable given the fact that the interaction does mix the states of opposite chirality and is the result of the vectorial nature of the coupling. The gapped CDW is a possible state for repulsive interactions only when $2V(2\vec{K}_0) < V(\vec{q})$ for small $\vec{q}$, which is not the case for local interactions.

Intranodal excitonic insulator.—Having established the instabilities in the internodal sector, we turn to those promoted by the first two terms in Eq. (2). For $V(\vec{q}) = \frac{g}{\Omega}$, we get

$$V = -\frac{g}{2\Omega}\sum_{\vec{k},\vec{k}'}(\vec{\Phi}^{1*}_{\vec{k}}\cdot\vec{\Phi}^{1}_{\vec{k}'} + \vec{\Phi}^{2*}_{\vec{k}}\cdot\vec{\Phi}^{2}_{\vec{k}'}), \quad (4)$$

with $\vec{\Phi}^1_{\vec{k}} = \hat{e}^1_{\vec{k}}(c^{L\dagger}_{\vec{k},+}c^{L}_{\vec{k},-} + c^{R\dagger}_{\vec{k},+}c^{R}_{\vec{k},-})$ and $\vec{\Phi}^2_{\vec{k}} = \hat{e}^2_{\vec{k}}(c^{L\dagger}_{\vec{k},+}c^{L}_{\vec{k},-} - c^{R\dagger}_{\vec{k},+}c^{R}_{\vec{k},-})$. Since $\hat{e}^1_{\vec{k}}$ only spans the southern hemisphere, azimuthal symmetry is preserved only about the $\hat{z}$ axes. This implies that there are four possible particle-hole instabilities for order parameters with the $\hat{e}^1_{\vec{k}}$ component: (i) chiral z EI, $\vec{\Delta}^L_{cz1} + \vec{\Delta}^R_{cz1} = \frac{g}{2\Omega}\langle\sum_{\vec{k}}\hat{e}^1_{\vec{k}}(c^{L\dagger}_{\vec{k},-n}c^{L}_{\vec{k},n} + c^{R\dagger}_{\vec{k},-n}c^{R}_{\vec{k},n})\rangle = (\Delta^L_{cz1} + \Delta^R_{cz1})(\frac{\hat{x}+i\hat{y}}{\sqrt{2}})$, (ii) polar z EI, $(\Delta^L_{pz1} + \Delta^R_{pz1})\hat{z}$, (iii) polar x EI, $(\Delta^L_{px1} + \Delta^R_{px1})\hat{x}$, and (iv) chiral x EI, $(\Delta^L_{cx1} + \Delta^R_{cx1})(\frac{\hat{y}+i\hat{z}}{\sqrt{2}})$. For $g > 3(\hbar v)^3/2\pi\Lambda^2$ there exists polar z EI which has the largest gap for the same interaction strength among these four states. At zero temperature we get $\Delta_{pz1} > \Delta_{cx1} > \Delta_{cz1} > \Delta_{px1}$ and $E_c^{pz1} < E_c^{cx1} < E_c^{cz1} < E_c^{px1}$ for the same interaction strength g larger than $6(\hbar v)^3/\pi\Lambda^2$ as shown in Fig. 3. By comparing it with Fig. 2 we see the polar z EI and the chiral CDW are equally energetically favorable among the six possible states aforementioned for a given interaction strength. None of these phases gap out the Weyl node.

For the order parameter of the particle-hole instabilities along the $\hat{e}^2_{\vec{k}}$ component, the order parameters have different signs between the two Dirac nodes and there are two possible EI states based on symmetry (no z component in $\hat{e}^2_{\vec{k}}$): (i) chiral EI, $\vec{\Delta}^L - \vec{\Delta}^R = \frac{g}{2\Omega}\langle\sum_{\vec{k}}\hat{e}^2_{\vec{k}}(c^{L\dagger}_{\vec{k},-n}c^{L}_{\vec{k},n} - c^{R\dagger}_{\vec{k},-n}c^{R}_{\vec{k},n})\rangle = (\Delta^L_{c2} + \Delta^R_{c2})(\frac{\hat{x}+i\hat{y}}{\sqrt{2}})$ with the signs fixed by setting $\Delta^R_{c2} = \Delta^L_{c2} \equiv \Delta_{c2}/2 > 0$ under the assumption of inversion symmetry, and (ii) polar EI, $(\Delta^L_{a2} + \Delta^R_{a2})\hat{x}$ with the same sign convention. For $g > (\hbar v)^3/\pi\Lambda^2$ there exists a chiral EI instability with a uniform gap. From Fig. 4 we

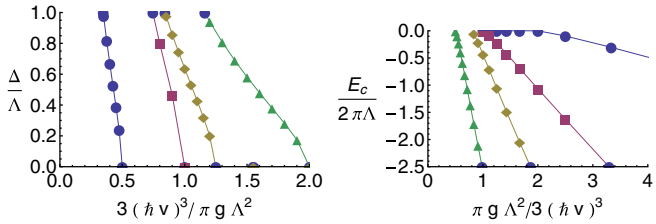

FIG. 3 (color online). Left: Order parameter magnitude as a function of inverse of the interaction strength for polar x EI Δ_{px1} (blue ○), chiral z EI Δ_{cz1} (purple □), chiral x EI Δ_{cx1} (brown ◇), and polar z EI Δ_{pz1} (green △). Right: Comparison of condensate energy E_c with $\mu = 0$ for aforementioned states as a function of the interaction strength.

see this state has the largest gap value compared with all other state for a given interaction strength. The chiral EI state is also more energetically favorable at zero temperature compared with the chiral CDW or polar z EI. For local repulsive interactions, the intranodal chiral excitonic insulator has the lowest critical coupling constant, opens a gap at the Weyl nodes, and has the lowest free-energy.

Ferromagnetism.—The chiral EI states mix particle and hole states which have opposite spin orientations in the noninteracting limit. Thus the ground state no longer has the spins aligned with their momenta. To evaluate the nature of the spin configuration we compute the expectation value of spin at momenta $\vec{k}$ for the occupied band. The result is that there exists a net polarization at each Weyl node. To understand the origin of this effect we first rotate the mean-field Hamiltonian back to the $\psi_{\vec{k},\sigma}$ basis. It takes the form

$$H_{\pm} = H_{0\pm} - \sum_{\vec{k}} \psi^{\dagger}_{\vec{k}\alpha} \vec{\Delta}' \cdot [\hat{e}^2_{\vec{k}} \hat{e}^2_{\vec{k}} \mp (\hat{e}^2_{\vec{k}} \times \vec{n}) \hat{e}^1_{\vec{k}}] \cdot \vec{\sigma}_{\alpha\beta} \psi_{\vec{k}\beta},$$

where $\vec{\Delta}' = \tilde{\Delta} \sin(\chi) \hat{l} + \tilde{\Delta} \cos(\chi) \hat{m}$, $\tilde{\Delta}$ is $|\vec{\Delta}_{c2} \cdot \hat{e}^2_{\vec{k}}|$, and χ is the corresponding phase. Under inversion $\hat{e}^1_{\vec{k}}$ does not change sign but $\hat{e}^2_{\vec{k}}$ does. Since we also go from one Weyl node to the other under inversion, the Hamiltonian preserves the symmetry. Averaging over polar and azimuthal angle the Hamiltonian is $\vec{\Delta}' \cdot \vec{\sigma}/2$ at both nodes. This is the origin of the magnetization in the chiral EI state and serves as a diagnostic of the state. An external magnetic field couples linearly to the order parameter leading to a lowering of the critical coupling, provided that it is smaller than the magnitude of the gap and no Landau levels are formed.

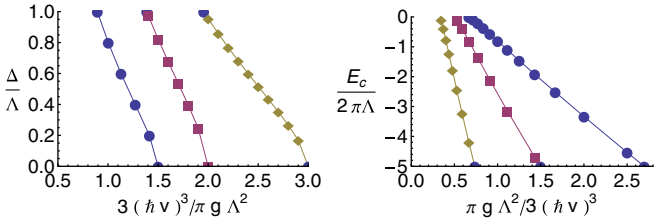

FIG. 4 (color online). Left: Order parameter magnitude as a function of inverse of the interaction strength for polar EI Δ_{p2} (blue ○), chiral CDW Δ_c (purple □), and chiral EI Δ_{c2} (brown ◇). Chiral CDW is shown here for comparison. Right: Comparison of condensate energy E_c with $\mu = 0$ for aforementioned channels as a function of the interaction strength. Chiral EI is the most energetically favorable among all states.

Discussion.—Our analysis focused on systems with two Weyl nodes. The TNI heterostructures [4] offer a simple realization where one can look for the excitonic phases reported here. PIs are another system where, in a regime of intermediate correlations, a Weyl semimetal with 24 nodes is conjectured to occur [3]. This implies that each Weyl node can couple to 12 other nodes with opposite chirality. On the other hand, the available phase space and the cutoff Λ will scale down. Whether the parameters end up being favorable to obtain the state is an open question that can only be answered once a Weyl semimetallic state is established and characterized. Nevertheless, the ongoing efforts to investigate systems with strong spin-orbit interactions promises to focus interest on exploring possible new correlated phases of matter.

Conclusion.—The interplay of strong spin-orbit coupling and repulsive interaction leads to novel excitonic phases in Weyl semimetals. The chiral nature of the low-energy excitations leads to a variety of possibilities, but for short-range interactions, only one of them opens a gap at the Weyl nodes. This is a consequence of the vectorial nature of the order parameter and shares a number of similarities with the physics of liquid ^{3}He. As such, it will be interesting to see if a nodal phase is favored over a fully gapped phase in any part of the phase diagram. Our chief conclusion is that, for local interactions, the ground state is a gapped ferromagnetic insulator, with the phase of the complex order parameter determining the direction of the ordered moment.

The authors acknowledge financial support by University of California at Riverside through the initial complement.

[1] J. C. Y. Teo, L. Fu, and C. L. Kane, Phys. Rev. B **78**, 045426 (2008); L. Fu, C. L. Kane, and E. J. Mele, Phys. Rev. Lett. **98**, 106803 (2007).
[2] R. Roy, Phys. Rev. B **79**, 195322 (2009); J. E. Moore and L. Balents, Phys. Rev. B **75**, 121306(R) (2007); B. A. Bernevig, T. L. Hughes, and S. C. Zhang, Science **314**, 1757 (2006).
[3] X. Wan, A. M. Turner, A. Vishwanath, and S. Y. Savrasov, Phys. Rev. B **83**, 205101 (2011).
[4] A. A. Burkov and L. Balents, Phys. Rev. Lett. **107**, 127205 (2011).
[5] A. A. Zyuzin, Si Wu, and A. A. Burkov, Phys. Rev. B **85**, 165110 (2012).

[6] J.-H. Jiang, Phys. Rev. A **85**, 033640 (2012).
[7] T. Meng and L. Balents, Phys. Rev. B **86**, 054504 (2012).
[8] K. Y. Yang, Y. M. Lu, and Y. Ran, Phys. Rev. B **84**, 075129 (2011).
[9] H. B. Nielsen and M. Ninomiya, Phys. Lett. **130B**, 389 (1983).
[10] V. Aji, Phys. Rev. B **85**, 241101 (2012).
[11] P. Hosur, S. A. Parameswaran, and A. Vishwanath, Phys. Rev. Lett. **108**, 046602 (2012).
[12] G. E. Volovik, *Universe in a Helium Droplet* (Oxford University Press, Oxford, 2003).
[13] T. Tsuneto, *Supercondutivity and Superfluidity* (Cambridge University Press, Cambridge, England, 1998).
[14] C. Kallin and A. J. Berlinsky, J. Phys. Condens. Matter **21**, 164210 (2009).
[15] W. Kohn, Phys. Rev. Lett. **19**, 439 (1967).
[16] See Supplemental Material at http://link.aps.org/supplemental/10.1103/PhysRevLett.109.196403 for evaluations of various critical coupling g_c.